Development 138, 3213-3224 (2011) doi:10.1242/dev.058693

The L6 domain tetraspanin Tm4sf4 regulates endocrine pancreas differentiation and directed cell migration

Keith R. Anderson[1,2], Ruth A. Singer[3], Dina A. Balderes[3], Laura Hernandez-Lagunas[2], Christopher W. Johnson[1,2], Kristin B. Artinger[1,2,*] and Lori Sussel[1,3,*]

SUMMARY

The homeodomain transcription factor Nkx2.2 is essential for pancreatic development and islet cell type differentiation. We have identified Tm4sf4, an L6 domain tetraspanin family member, as a transcriptional target of Nkx2.2 that is greatly upregulated during pancreas development in Nkx2.2$^{-/-}$ mice. Tetraspanins and L6 domain proteins recruit other membrane receptors to form active signaling centers that coordinate processes such as cell adhesion, migration and differentiation. In this study, we determined that Tm4sf4 is localized to the ductal epithelial compartment and is prominent in the Ngn3^{+} islet progenitor cells. We also established that pancreatic *tm4sf4* expression and regulation by Nkx2.2 is conserved during zebrafish development. Loss-of-function studies in zebrafish revealed that *tm4sf4* inhibits α and β cell specification, but is necessary for ε cell fates. Thus, Tm4sf4 functional output opposes that of Nkx2.2. Further investigation of how Tm4sf4 functions at the cellular level in vitro showed that Tm4sf4 inhibits Rho-activated cell migration and actin organization in a ROCK-independent fashion. We propose that the primary role of Nkx2.2 is to inhibit Tm4sf4 in endocrine progenitor cells, allowing for delamination, migration and/or appropriate cell fate decisions. Identification of a role for Tm4sf4 during endocrine differentiation provides insight into islet progenitor cell behaviors and potential targetable regenerative mechanisms.

KEY WORDS: Nkx2.2, Tm4sf4, Pancreas, Islet cell, Differentiation, Mouse, Zebrafish

INTRODUCTION

The pancreas develops through a series of intricate steps involving highly coordinated signaling, transcriptional and morphological events that are tightly regulated to produce mature ductal, exocrine and endocrine tissue compartments (for reviews, see Gittes, 2009; Jorgensen et al., 2007; Murtaugh, 2008; Oliver-Krasinski and Stoffers, 2008; Puri and Hebrok, 2010). Despite the identification of many different transcriptional components that are important for pancreas development, the downstream mechanisms that ultimately lead to specification or differentiation of pancreatic cell types are still not well understood.

During mouse pancreatic development, the critical stage of islet cell differentiation occurs between embryonic day (e) 12.5 and e15.5 (Oliver-Krasinski and Stoffers, 2008; Rutter et al., 1968), at which time endocrine progenitor cells, which are demarcated by their expression of the basic helix-loop-helix transcription factor Ngn3 (Neurog3 – Mouse Genome Informatics), localize and multiply in the branched epithelial pancreatic ducts. As the Ngn3^{+} population differentiates, Ngn3 becomes downregulated once differentiating endocrine cells lose polarity, delaminate and migrate from the ducts into the surrounding mesenchyme and developing acinar environment (Gouzi et al., 2011; Slack, 1995). Identifying the extracellular factors that are important for maintenance of the progenitor population by regulating adhesion, migration and/or differentiation is crucial for understanding pancreas development, as well as for potential therapeutic design.

[1]Molecular Biology Program, University of Colorado Denver, Aurora, CO 80045, USA. [2]Department of Craniofacial Biology, University of Colorado Denver Health Sciences Center, Aurora, CO 80045, USA. [3]Department of Genetics and Development, Columbia University, New York, NY 10032, USA.

*Authors for correspondence (Kristin.artinger@ucdenver.edu; lgs2@columbia.edu)

Accepted 11 May 2011

In zebrafish, many aspects of islet development are similar to those in the mouse. The posterior (dorsal) bud gives rise to the principal endocrine islet and appears at 24 hours post-fertilization (hpf) whereas the anterior (ventral) anlage is not evident until 40 hpf and develops into exocrine, ductal and some endocrine tissues (Field et al., 2003; Tiso et al., 2009). It has been proposed that, similar to mouse, Notch-responsive cells initiate a secondary transition in the developing zebrafish pancreas (Parsons et al., 2009). Although zebrafish embryos lack *ngn3* (*neurog3* – Zebrafish Information Network) expression during early pancreas development (Zecchin et al., 2007), endocrine precursors express the transcription factor *sox4b* in a domain ventral to the developing principal islet at 24 hpf (Mavropoulos et al., 2005; Soyer et al., 2010). *sox4b* is expressed transiently in endocrine precursors and responds to Notch signaling in the same manner as *Ngn3* in mice (Mavropoulos et al., 2005).

Although the endocrine progenitor program may be initiated by different transcription factor(s) in mouse and zebrafish, many of the upstream and downstream transcription factors or signaling molecules have conserved roles in the two organisms (Biemar et al., 2001; Kinkel and Prince, 2009). The homeodomain transcription factor Nkx2.2 is crucial for both mouse and zebrafish islet cell differentiation. *Nkx2.2*$^{-/-}$ mice completely lack β cells, have an 80% decrease in α cells and a modest reduction in PP cells. Conversely, ghrelin^{+} (ε) cells are significantly increased and fill the islets in *Nkx2.2*$^{-/-}$ mice (Prado et al., 2004; Sussel et al., 1998). These islet cell differentiation defects are conserved in zebrafish pancreas organogenesis when *nkx2.2a* translation is blocked (Pauls et al., 2007).

Analysis of the genome-wide expression changes that occur in the mouse *Nkx2.2*$^{-/-}$ pancreas at onset of the secondary transition identified a tetraspanin-like protein, Tm4sf4, as a direct target of Nkx2.2 that is highly upregulated in *Nkx2.2*$^{-/-}$ pancreata (Anderson et al., 2009a; Hill et al., 2011). Tetraspanins are defined by their similar protein topology and predicted tertiary structure. They can

interact with other tetraspanins, integrins, growth factor receptors and signaling molecules that occur both extracellularly and intracellularly to form large tetraspanin-enriched microdomains (TEMs). TEMs have been shown to function as signaling centers crucial for adhesion, migration and proliferation (Hemler, 2005; Hemler, 2008; Yunta and Lazo, 2003).

Tm4sf4 is classified as a member of the more divergent tetraspanin L6 domain family owing to a lack of characteristic cysteine residue motifs in the EC2 extracellular domain (Wright et al., 2000). Other members of the L6 family include *Tm4sf1* (*L6-Ag*), *Tm4sf5* and *Tm4sf18* (*L6D*) (Wright et al., 2000). *Tm4sf1* and *Tm4sf5* have been shown to be upregulated in multiple tumors, have roles in epithelial-to-mesenchymal transition (EMT) and affect migratory mechanisms crucial to cancer invasion and metastasis (Kao et al., 2003; Lee et al., 2008; Marken et al., 1992; Muller-Pillasch et al., 1998; Muschel and Gal, 2008; Storim et al., 2001). Unlike its homologs, little mechanistic information is known about Tm4sf4. Tm4sf4 levels appear to increase when non-dividing epithelial cells differentiate and migrate out of intestinal crypts (Wice and Gordon, 1995). In the liver, Tm4sf4 is expressed in non-dividing hepatocytes that retain high proliferative potential when given the correct stimulus, and is upregulated during liver injury (Liu et al., 2001; Qiu et al., 2007). In the context of Nkx2.2 loss of function, when endocrine differentiation is severely disrupted, *Tm4sf4* is highly upregulated. In this study, we describe novel roles for *Tm4sf4* in regulating islet cell fates and inhibiting cellular migration that might provide a principal mechanism for Nkx2.2 function in the pancreas.

MATERIALS AND METHODS

Animals

Nkx2.2$^{+/-}$ heterozygous mice (Sussel et al., 1998) and *Ngn3*$^{+/EGFP}$ (Lee et al., 2002) heterozygous mice were maintained on Swiss Black (Taconic) backgrounds. Genotyping of mice and embryos was performed as previously described (Sussel et al., 1998; Lee et al., 2002). Mice were housed and treated according to Columbia University and UCD-AMC IACUC approval protocols.

Zebrafish were maintained and embryos staged according to standard protocols (Kimmel et al., 1995). For initial experiments screening morpholino phenotypes and function, wild-type AB, TAB and EKK strains were used. All subsequent experiments were done with single mating wild-type EKK embryos.

RNA in situ hybridization (ISH)

Mouse RNA ISH was performed as previously described (Prado et al., 2004). A full-length mouse Tm4sf4 cDNA clone (Open Biosystems/ThermoScientific, AL, USA) was used to generate the antisense probe. Pictures were acquired on a Leica CTR 5000 with 20× magnification.

Zebrafish whole-mount ISH was performed as described by Thisse and Thisse (Thisse and Thisse, 2008), digoxigenin (DIG)-labeled antisense RNA probes: *tm4sf4* (PCR cloned: Forward 5′-ATCATGTGCTCTG-GAAATTTCGCC-3′, Reverse 5′-TTACTTTATTCCTTGCAGCAGCCG-3′); *insulin*, *glucagon*, *somatostatin and ghrelin* [synthesized from cDNAs provided by Chris Wright (Vanderbilt University, TN, USA)] and *sox4b* [Marianne Voz (GIGA, Sart-Tilman, Belgium)]. Images were acquired on an Olympus BX51 with 20× magnification.

Immunofluorescence

Mouse immunofluorescence was performed on frozen 8 μm sections. Images were acquired on a Leica DM5500. For cell staining, cells were grown and fixed on coverslips or Boyden Chamber filters and images acquired on a Zeiss META LSM510. Rhodamine phalloidin was incubated for the last 30 minutes of the secondary antibody incubation.

Whole-mount 48 hpf zebrafish embryos were fixed in 4% paraformaldehyde (PFA) for 1 hour at 25°C. Embryos were deyolked, followed by 2×5 minute water washes and 1 hour in blocking solution [2% goat serum, 2% BSA, 1% DMSO, 0.2% Triton X-100, in 1× PBS]. Embryos were imaged on a Zeiss META LSM 510. Confocal *z*-stacks were taken every 2 μm and compiled by 3D rendering using Imaris software (Bitplane Scientific Software, MN). Glucagon- and Insulin- positive cells were counted per islet, n=6 for both uninjected and *tm4sf4* morphant conditions.

Antibodies and markers used were: goat anti-CpA (1:800; R&D Systems, MN, USA), mouse anti-FLAG (1:500; Sigma, MO, USA); rabbit anti-ghrelin (1:800; Phoenix Pharmaceuticals, CA, USA); guinea pig anti-glucagon (1:1000; Millipore, MA, USA); mouse anti-Glucagon (1:300; Sigma); guinea pig anti-insulin (1:1000 or 1:200; Millipore); rabbit anti-Sox9 (1:1000; Chemicon); DBA-lectin (1:100; Vector Laboratories, CA, USA); Rhodamine-phalloidin (1:100; Invitrogen, CA, USA); donkey anti-guinea pig-Cy3 (1:200; Jackson ImmunoResearch, PA, USA); donkey anti-guinea pig-Cy5 (1:300; Jackson ImmunoResearch); donkey anti-rabbit-Cy2 (1:200; Jackson ImmunoResearch); donkey anti-mouse-Cy2 (1:200; Jackson ImmunoResearch) and DAPI (1:1000; Invitrogen).

Morpholinos

Injection bolus size was measured on a 1 mm ruled:0.01 mm division micrometer (12-561-SM1, Sigma). Ten ng of *nkx2.2*atgMO (MOnk-5UTR, 5′-TGGAGCATTTGATGCAGTCAAGTTG-3′) (Pauls et al., 2007), 4-8 ng of Translation (*tm4*atgMO, 5′-AATTTCCAGAGCACATGATTG-AGTC-3′) or splice blocking (*tm4*splMO, 5′-GTTATTGTTTTTCTCAC-CGCAAATC-3′) morpholinos (Gene Tools, OR, USA) were injected into embryos at the 1- to 4-cell stage. Injected embryos were screened by rhodamine or cascade blue dextran prior to experimental analysis.

Real-time quantitative PCR (qRT-PCR)

RNA from fluorescence-activated cell (FAC) sorted populations (White et al., 2008) or tissue culture cells were isolated with an RNeasy Mini Kit (Qiagen, CA, USA). cDNA was transcribed using a Superscript III Kit (Invitrogen). Pre-designed mouse *Tm4sf4* (Mm00523755_m1, Life Technologies, CA, USA) and custom *Ngn3* primer/probe Taqman assays were used to measure mRNA expression levels and were normalized to the internal control gene, *cyclophilin B*, with a custom Taqman primer/probe set. Relative quantification used a standard curve from wild-type cDNA. For zebrafish samples, ten wild type and ten *tm4sf4* morphants for each time point were collected and pooled into one sample for each condition. Samples were processed as described above. Each gene of interest was normalized to β-*actin* expression and the ΔΔCt method (Life Technologies) was used for relative quantification. Mouse and zebrafish sequences are listed in Table S1 in the supplementary material.

Cell culture and Boyden chamber migration assays

mPacL20, NIH 3T3 and 293T cells were cultured in DMEM with 10% FBS. For Tm4sf4-FLAG overexpression, the *Tm4sf4* cDNA (MMM1013-65619, Open Biosystems) was cloned into pCMV Sport6 with a reverse primer containing FLAG nucleotides. For overexpression, cells were transfected with 0.8 μg Tm4sf4-FLAG and lipofectamine 2000 (NIH 3T3-5:1 ratio, 293T-4:1 ratio) (Invitrogen). For siRNA knockdown, mPacL20 cells were transfected with 10 pmol predesigned siControl (scrambled siRNA not known to degrade any RNA) or siTm4sf4 (sc-154303, Santa Cruz Biotechnology, CA, USA) and 1 μl lipofectamine 2000. At 40 hours post-transfection, cells were serum starved for 30 minutes, trypsinized and added to medium lacking FBS. Half the cells were added to the Boyden chamber insert (ECM508, Millipore), which was then added to a 24-well plate containing medium with FBS. Cells were allowed to migrate for 24 hours before fixing and staining nuclei. Three 20× magnification fields were imaged per well for each condition in triplicate (total n=9), and the number of migrated cells was counted manually. In knockdown cells, morphology differences were identified by broadly spread cells with intense and disorganized actin cytoskeleton, n=6.

For Rho family activator or inhibitor treatments, mPacL20 cells were allowed to adhere to the insert membrane for 2 hours prior to drug additions with the following final concentrations: 0.25 units/ml Rac/Cdc42 activator (CN02, Cytoskeleton, Denver, CO, USA), 1 μg/ml Rho Inhibitor/cell permeable C3 transferase (CT04, Cytoskeleton), 100 μM ROCK inhibitor Y-

27632 (Y0503, Sigma-Aldrich), 0.2 or 0.4 μg/ml pan-small GTPase inhibitor Toxin B (616377, EMD Chemicals, Gibbstown, NJ, USA). Cell migration occurred for 18 hours prior to cell fixation and quantification.

RESULTS

Tm4sf4 is expressed in early pancreatic epithelium and is highly upregulated in *Nkx2.2*$^{-/-}$ mice

In wild-type pancreata, *Tm4sf4* mRNA is expressed at low levels throughout the central trunk domain (Anderson et al., 2009a). *Tm4sf4* mRNA is expressed in the pancreatic epithelium as early as e10.5 (Fig. 1A). In the absence of *Nkx2.2*, *Tm4sf4* became highly upregulated at e10.5, e12.5 and e15.5 (Fig. 1A,C,F,I,K,O). Within the endocrine compartment, *Tm4sf4* was only co-expressed with a rare number of insulin^{+} cells (Fig. 1S), and high *Tm4sf4* mRNA-expressing (Tm4sf4^{HI}) cells did not appear to overlap with glucagon or ghrelin protein expression in wild-type or *Nkx2.2*$^{-/-}$ pancreata (Fig. 1A-D,F,G,I,J). The lack of correlative localization with ghrelin^{+} cells in the Nkx2.2$^{-/-}$ pancreata suggests that upregulation of *Tm4sf4* is not due to elevated numbers of ε cells (Anderson et al., 2009a). Analysis of Tm4sf4 mRNA expression with carboxypeptidase A (CpA) immunohistochemical staining also suggested that CpA^{-} ductal trunk cells are enriched with Tm4sf4, with lower expression visible in the CpA^{+} distal tip domains and exocrine tissue (Fig. 1S,T). Immunofluorescence staining for the ductal markers DBA-lectin and Sox9 on adjacent sections to *Tm4sf4* mRNA expression confirmed enrichment of the Tm4sf4 expression domain in the developing ductal network (Fig. 1E,F,H,I,K,L,O,P).

Based on the predominant localization of high *Tm4sf4* mRNA levels to the pancreatic ductal regions, we hypothesized that *Tm4sf4*^{HI} is localized to the endocrine progenitor cell population. Using fluorescence-activated cell sorting (FACS) technology on Ngn3-EGFP mouse pancreata (Lee et al., 2002), GFP^{+} (Ngn3^{+}, 5.9%) and GFP^{-} (Ngn3^{-}, 91.6%) cell populations were collected from e14.5-16.5 pancreata at the peak of Ngn3 expression and cell specification (Fig. 2A). In agreement with the expression analysis, we found that the Ngn3^{+} endocrine progenitor population was highly enriched with *Tm4sf4* mRNA during the secondary transition (Fig. 2B). Ngn3$^{-/-}$ mouse pancreata (Lee et al., 2002), which lack all endocrine cell populations, expressed similar levels of *Tm4sf4* (Fig. 2C-E), to further support the localization of Tm4sf4 expression in the central ductal (non-endocrine) domains of the pancreas.

Previous studies have shown that *Tm4sf4* is expressed in both liver and intestine (Liu et al., 2001; Qiu et al., 2007; Wice and Gordon, 1995). Although *Nkx2.2* is expressed in a subset of intestinal enteroendocrine cells and has a functional role in cell fate choices (Desai et al., 2008), *Tm4sf4* intestinal mRNA expression appeared to be unaltered in *Nkx2.2*$^{-/-}$ mice (Fig. 1N,R; see Fig. S1

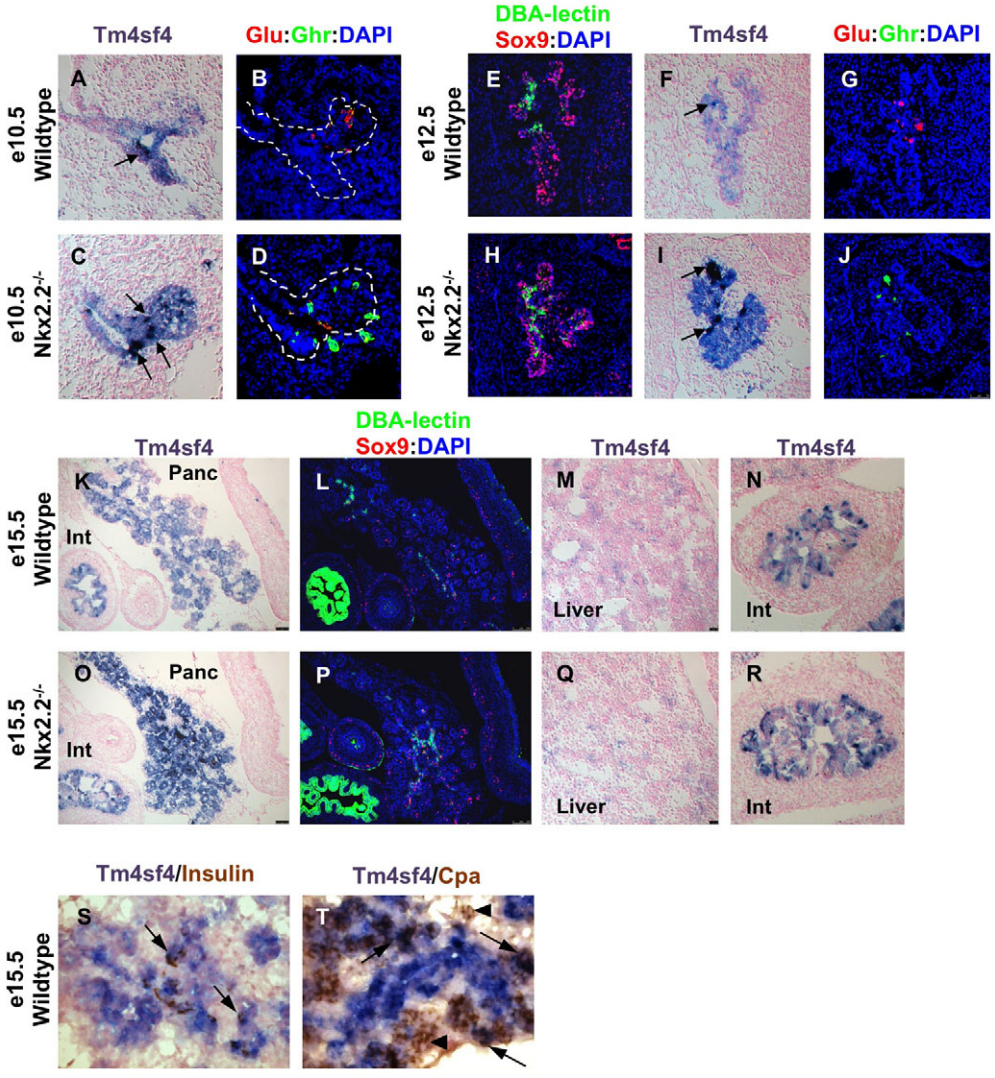

Fig. 1. *Tm4sf4* is expressed in the early mouse pancreatic epithelium and is upregulated in *Nkx2.2*$^{-/-}$ pancreata. (**A-T**) Pancreatic *Tm4sf4* expression was assessed by in situ hybridization at e10.5 (A,C), e12.5 (F,I) and e15.5 (K,O,S,T) in both wild-type and *Nkx2.2*$^{-/-}$ mice. Colocalization of *Tm4sf4* with glucagon (red), Sox9 (red), lectin (green), ghrelin (green), insulin (brown) and CpA (brown) was analyzed on adjacent sections (B,D,E,G,H,J,L,P,S,T). Examples of *Tm4sf4*^{HI} regions are identified by arrows. Dashed lines in B and D encircle the pancreatic epithelium. *Tm4sf4* expression was analyzed in the liver (M,Q) and intestine (N,R) of wild-type and *Nkx2.2*$^{-/-}$ mice. All images are 20× magnification, except K,L,O,P which are 10× and S,T which are 40×. Int, intestine; Panc, pancreas.

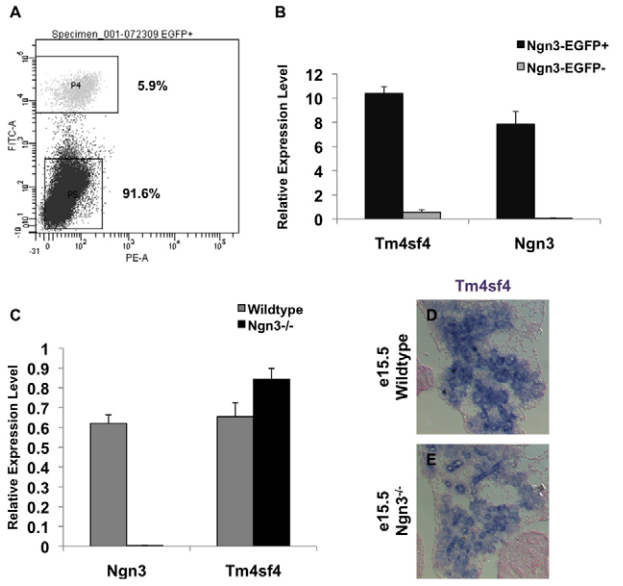

Fig. 2. Mouse Ngn3^{+} pancreatic endocrine progenitor cells are enriched with *Tm4sf4*. (**A**) Fluorescence-activated cell sorting (FACS) plot showing the gates and percentages obtained for GFP^{+} and GFP^{-} populations. (**B**,**C**) qRT-PCR for *Tm4sf4* and *Ngn3* mRNA from Ngn3^{+} (black) and Ngn3^{-} (gray) cells from FACS experiments (B), and wild-type (gray) or Ngn3$^{-/-}$ (black) pancreata (C). Error bars represent s.e.m. (**D**,**E**) *Tm4sf4* in situ hybridization analysis on e15.5 wild-type (D) and Ngn3$^{-/-}$ (E) pancreata.

in the supplementary material). Consistent with the absence of Nkx2.2 expression in the liver, *Tm4sf4* mRNA levels were unchanged in the liver of *Nkx2.2*$^{-/-}$ mice (Fig. 1M,Q). We also determined that the other closely related L6 family members were not expressed at high levels in the pancreas (see Fig. S1 in the supplementary material) and did not display elevated expression in *Nkx2.2*$^{-/-}$ pancreata (see Fig. S1 in the supplementary material) (Hill et al., 2011). These findings suggest that regulation of *Tm4sf4* by Nkx2.2 is specific to the pancreatic domain and is unique among its L6 counterparts.

The *Tm4sf4* gene and expression pattern is conserved in zebrafish

To determine the function of *tm4sf4* in the developing pancreas, we used zebrafish to knockdown *tm4sf4* using antisense morpholino (MO) technology. We identified a single zebrafish Tm4sf4 ortholog (zgc:92479) with 79% similarity to mouse Tm4sf4 (Fig. 3A). Performing temporal qRT-PCR analysis, we determined that *tm4sf4* expression initiates at 10 hpf and increases until 168 hpf, with spikes of expression occurring at 20.5, 48 and 144 hpf (Fig. 3B,C). The first spike in expression corresponds to a time period (15-24 hpf) at which endocrine progenitor markers are being induced and β cells are specified (Biemar et al., 2001). Furthermore, 18-21 hpf represents a stage when the endoderm first begins to organize radially near pancreatic and liver domains, forming what will later become the polarized gut tube (Wallace and Pack, 2003). Similar to murine *Tm4sf4*, zebrafish *tm4sf4* was expressed in liver, intestine and pancreas of 48 hpf embryos (Fig. 3D).

A conserved role for *Nkx2.2* in pancreas gene regulation, islet specification and duct morphogenesis has previously been shown in zebrafish (Anderson et al., 2009a; Pauls et al., 2007). To determine whether regulation of *Tm4sf4* by Nkx2.2 is also conserved in zebrafish, we assessed *tm4sf4* expression in *nkx2.2*MO-injected embryos. We confirmed that the *nkx2.2a* translation blocking morpholino was functional by measuring *insulin* and *ghrelin* mRNA levels at three stages during pancreas development. As previously described (Pauls et al., 2007), *insulin* was reduced approximately twofold at 52 hpf; however, we also showed this reduction to be apparent as early as 19.5 hpf (Fig. 3H). We determined that *ghrelin* is also increased by approximately twofold, as shown by Pauls et al. (Pauls et al., 2007), and that this increase in *ghrelin* occurs by 28 hpf (Fig. 3I). Similar to mice, morpholino knockdown of *nkx2.2a* resulted in increased *tm4sf4* expression specific to pancreas as seen by ISH at 36 hpf (Fig. 3E,F). When mRNA levels were measured by qRT-PCR, *tm4sf4* was increased in *nkx2.2a* morphant embryos by approximately threefold at 19 hpf, ~1.7-fold at 28 hpf, but appeared to be unchanged by 52 hpf (Fig. 3G). This apparent loss of a *tm4sf4* phenotype probably results from analyzing mRNA extracted from whole zebrafish embryos; the high and unaltered expression of Tm4sf4 in the developing liver and intestine could mask any pancreas-specific phenotypes. For a summary of morpholino penetrance see Table 1.

tm4sf4 inhibits β cell specification during zebrafish pancreas development

To determine whether *tm4sf4* plays a role during pancreas development, we used a translation-blocking morpholino (Tm4atgMO) and a splice-blocking morpholino (Tm4splMO, designed against the exon2-intron2 boundary) to knockdown *tm4sf4* expression globally throughout early zebrafish embryogenesis. Using the splice-blocking morpholino, we assessed efficiency of knockdown by detecting the appearance of aberrantly spliced products that would result in severely truncated or altered amino acid sequence (see Fig. S2 in the supplementary material). Injections of a nonsense control morpholino had no effect on hormone, transcription factor or *tm4sf4* expression analyzed by qRT-PCR or ISH (data not shown).

We hypothesized that loss of *tm4sf4* would lead to an increase in insulin-producing β cells because *Nkx2.2*$^{-/-}$ mouse pancreata contain no β cells, *tm4sf4* is highly upregulated and these phenotypes are conserved in the *nkx2.2a* morphant zebrafish embryos. Indeed, knockdown of *tm4sf4* by both Tm4atgMO and Tm4splMO resulted in a significant increase in *insulin* mRNA expression and β cell numbers within the pancreas at 30 hpf by ISH in a dose-dependent manner (see Fig. S3 in the supplementary material). The splice-blocking morpholino (Tm4splMO) was used for all subsequent experiments to allow quantification of knockdown via qRT-PCR. We confirmed that wild-type *tm4sf4* transcript was reduced by 50-75% when using 5 ng of the Tm4splMO morpholino (Fig. 4Q). Expression of the liver marker *hhex* and intestine marker *foxa3* appeared to be unaffected (data not shown). To ensure that the phenotype was specific to knockdown of Tm4sf4, we showed that *tm4sf4* mRNA co-injected with Tm4splMO could rescue the β cell phenotype and significantly reduce the number of β cells compared with uninjected embryos (see Fig. S3 in the supplementary material).

The phenotype associated with loss of *tm4sf4* function was analyzed by measuring endocrine hormone RNA levels at three consecutive stages during pancreas development (16.5-21 hpf, 24-30 hpf and 48-52 hpf). Using ISH analysis, we observed a persistent and significant twofold increase in *insulin* mRNA expression across the pancreatic developmental time points,

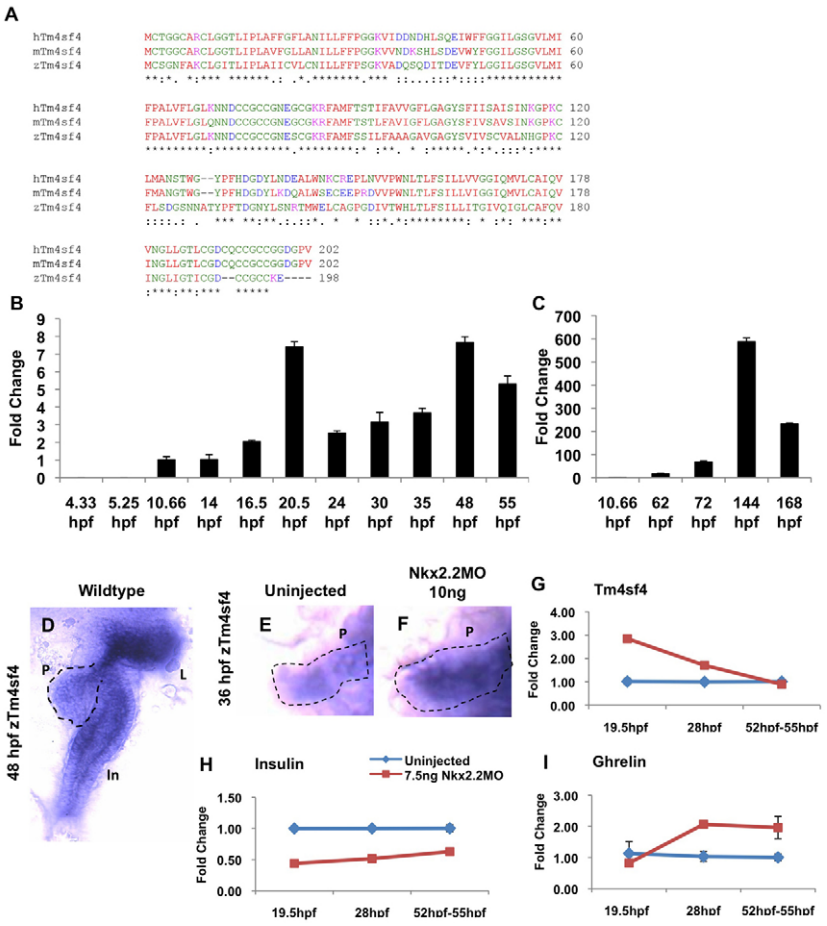

Fig. 3. The *tm4sf4* gene and regulation by *nkx2.2a* is conserved in zebrafish. (**A**) CLUSTAL W species alignment between human, mouse and zebrafish Tm4sf4. Identical (*), highly conserved (:) and weakly conserved (.) amino acids are indicated. Small/hydrophobic residues (red), acidic residues (blue), basic residues (magenta), hydroxyl/amine/basic residues (green) are shown. (**B**,**C**) Temporal qRT-PCR *tm4sf4* mRNA analysis of early (B) and late (C) stage zebrafish embryos. (**D-F**) *tm4sf4* in situ hybridization on wild-type (D,E) and *nkx2.2a* morphant (F) embryos. In, intestine; L, liver; P, pancreas. Images taken at 20× magnification. (**G-I**) qRT-PCR comparing uninjected (blue) and *nkx2.2a* morphant (red) embryo expression of *tm4sf4* (G), *insulin* (H) and *ghrelin* (I). Error bars represent s.e.m.

beginning at 16.5 hpf, soon after β cells are initially specified (Fig. 4A). ISH for *insulin* on 20.5 hpf embryos confirmed an increase in the number of *insulin*$^+$ cells (Fig. 4B,C). Between 15 hpf and 24 hpf, bilaterally specified β cells migrate to form a tight cluster adjacent to the midline (Biemar et al., 2001; Kim et al., 2005; Kinkel et al., 2008). Interestingly, the larger β cell population in *tm4sf4* morphant embryos appeared less clustered and extended more anteriorly than that of their uninjected counterparts (Fig. 4B,C). Quantification of insulin$^+$ β cells by immunofluorescence revealed a significant 1.4-fold increase in β cells per islet in *tm4sf4* morphants at 52 hpf (Fig. 5A-C). Similar results were observed in Tg(*insulin*::dsRed/*glucagon*:GFP) zebrafish (provided by R. Anderson and D. Stainier, University of California, San Francisco, CA, USA) at 30 hpf (data not shown). It remains possible that the increase in β cells is due to an increase in proliferation of differentiated β cells rather than to an increase in specification; however, temporal analysis suggests that the increase in *insulin* mRNA occurs early and does not continue to expand over time (Fig. 4A). In addition, we performed 5-ethynyl-2′-deoxyuridine (EdU) incorporation at 30 hpf to label cells actively in S phase of the cell cycle. Morphant embryos displayed no change in EdU$^+$ cells within the pancreatic insulin$^+$ population or the entire pancreatic domain when compared with uninjected embryos (Fig. 5F,G). Similarly, co-staining of Insulin and Phospho-histone H3 (PH3) on 20.5 hpf embryos did not identify proliferating PH3$^+$/Insulin$^+$ cells (data not shown). These findings suggest that knockdown of *tm4sf4* increases β cell number via increased specification or differentiation.

Table 1. Summary of in situ hybridization phenotypic analysis.

Gene	Morpholino	Age	Number of uninjected clutchmates	Number of morphant embryos with phenotypes/total number of injected embryos
tm4sf4	Nkx2.2MO	36 hpf	10	9/12 (75%)
insulin	Tm4sf4MO	20.5 hpf	10	9/10 (90%)
insulin	Tm4sf4MO	30 hpf	26	32/34 (94%)
insulin	Tm4sf4MO	50 hpf	134	122/146 (83.6%)
glucagon	Tm4sf4MO	20.5 hpf	8	8/8 (100%)
glucagon	Tm4sf4MO	50 hpf	59	3/64 (4.7%)
somatostatin	Tm4sf4MO	48 hpf	29	2/23 (8.7%)
ghrelin	Tm4sf4MO	48 hpf	10	5/6 (83.3%)
sox4b	Tm4sf4MO	18 hpf	4	4/4 (100%)

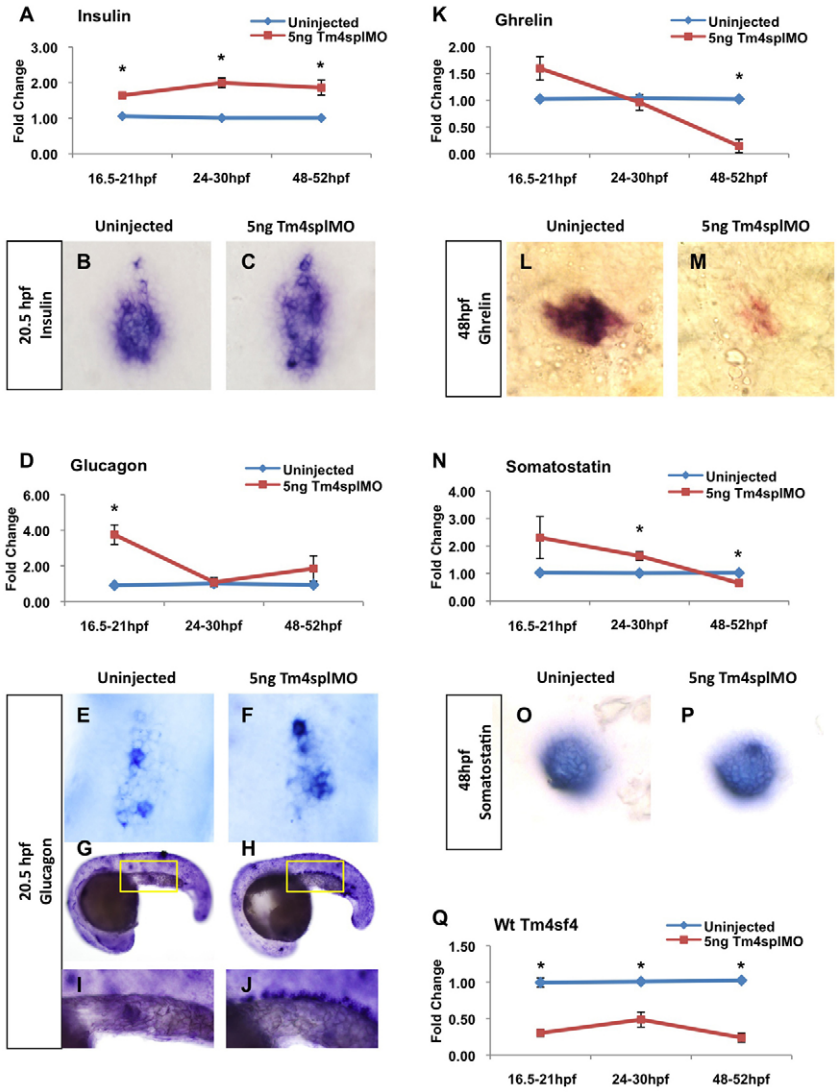

Fig. 4. *tm4sf4* inhibits α and β cell specification, and is necessary for ε cell fates. (**A-P**) Hormone mRNA levels were measured by qRT-PCR comparing uninjected (blue) and *tm4sf4* morphant (red) zebrafish embryos: *insulin* (A), *glucagon* (D), *ghrelin* (K), *somatostatin* (N). Hormone mRNA expression pattern was determined by in situ hybridization comparing uninjected and *tm4sf4* morphant embryos at 20.5 hpf for *insulin* (B,C) and *glucagon* (E-J), and at 48 hpf for *ghrelin* (L,M) and *somatostatin* (O,P). All images were taken at 40× magnification except G,H taken at 10×; yellow boxes represent areas enlarged in I and J. (**Q**) Knockdown efficiency of Tm4splMO was determined at all stages. Error bars represent s.e.m. *P<0.05.

tm4sf4 inhibits α cell specification during zebrafish pancreas and intestinal development

We determined that *glucagon* transcript levels were significantly elevated fourfold in *tm4sf4* morphant embryos by 16.5 hpf (Fig. 4D) and that by 20.5 hpf, pancreatic α cell number appeared increased, similar to that of β cells (Fig. 4E,F). However, the large early increase in *glucagon* mRNA disappeared by 24 hpf and remained unchanged compared with uninjected embryos up to 52 hpf (Fig. 4D). At 52 hpf, we confirmed that α cell numbers were unaltered in *tm4sf4* morphant embryos (Fig. 5A,B,D). Upon closer analysis of the trunk domain at 20.5 hpf, the *tm4sf4* morphant embryos contained a large midline stream of *glucagon*$^+$ cells along the developing intestinal tract, posterior to the pancreas (Fig. 4H,J). These cells underwent apoptosis by 28 hpf (Fig. 5H-K), suggesting that the intestinal *glucagon*$^+$ population in morphant embryos is transient and might explain the lack of a *glucagon* phenotype at later stages (Fig. 4D). *Glucagon*$^+$ cells within the intestine of uninjected clutch mates at 20.5 hpf were not detected (Fig. 4G,I). The emergence of *glucagon*$^+$ cells at this stage could be due to mis-specification of pancreatic α cells in the intestine or unregulated differentiation of enteroendocrine cells. However, we have only detected intestinal *tm4sf4* expression within a short section of the developing gut immediately posterior to the liver and pancreas (Fig. 3B). It remains possible that α cells, *glucagon*$^+$ intestinal cells, or their precursors, are born more anteriorly and migrate posteriorly within the developing gut tube of *tm4sf4* morphant embryos.

tm4sf4 is necessary for ε cell differentiation during zebrafish pancreas development

We determined whether Tm4sf4 also functions downstream of Nkx2.2 to regulate *ghrelin*-expressing ε cells. Consistent with the increase of α and β cells, *ghrelin* mRNA expression was decreased in *tm4sf4* morphant embryos when compared with uninjected embryos at 48 hpf (Fig. 4K). Although it has recently been suggested that *ghrelin*-expressing cells are present as early as 22 hpf (Soyer et al., 2010), *ghrelin* mRNA expression was not significantly changed until 48 hpf in *tm4sf4* morphants (Fig. 4K). However, as wild-type *ghrelin* levels are extremely low prior to 48 hpf, it remains possible that detection of a decrease at these early stages might be challenging. Even by 48 hpf, the zebrafish pancreas contains a relatively low number of cells expressing *ghrelin* (Fig. 4L) (Pauls et al., 2007). At 48 hpf, *tm4sf4* morphant zebrafish had significantly fewer *ghrelin*-expressing cells (Fig. 4L,M, Fig. 5E).

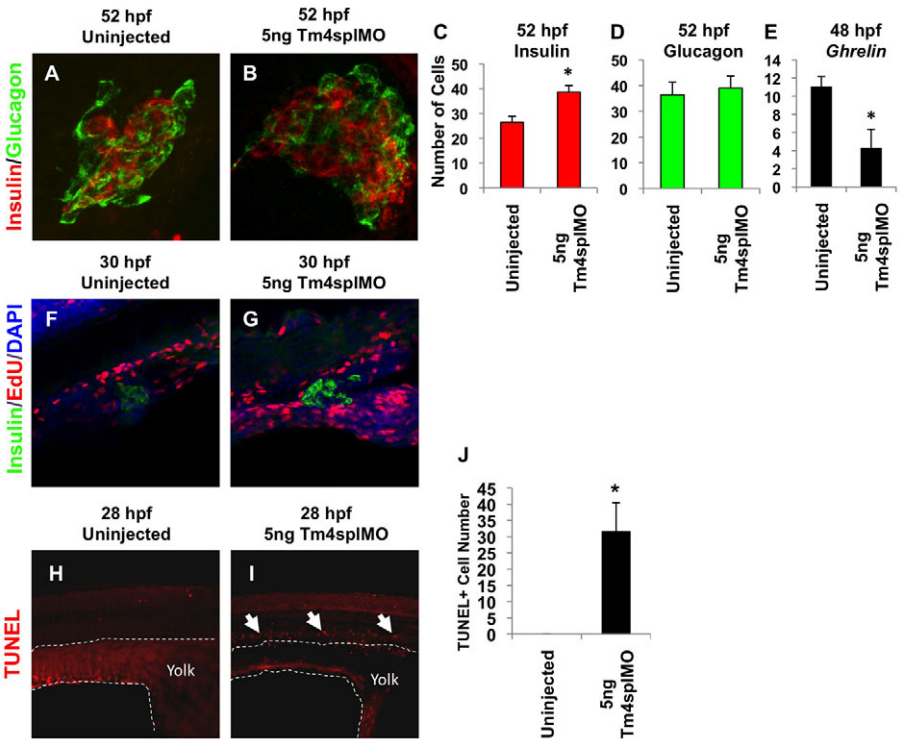

Fig. 5. β cells are increased independently of proliferation, ε cells are decreased and aberrant α cells undergo apoptosis as a consequence of *tm4sf4* loss.
(**A**,**B**) Immunofluorescence of insulin (red) and glucagon (green) in uninjected (A) and *tm4sf4* morphant (B) zebrafish embryos at 52 hpf. Confocal images were taken at 25× magnification with 2× digital zoom. (**C-E**) Total β (C) and α (D) cells were counted from confocal *z*-stacks (n=6). Total ε cells (E) were counted from in situ hybridization 20× images (n=6). (**F**,**G**) β cell proliferation was assessed by confocal microscopy of EdU (red) incorporation and immunofluorescence for insulin (green) in uninjected (F) and *tm4sf4* morphant (G) embryos. (**H-J**) TUNEL assay to assess apoptotic cells in the presumptive intestine of 28 hpf embryos. Arrows indicate TUNEL$^+$ cells. Dashed line delineates the yolk. Error bars represent s.e.m. *P<0.05.

Pancreas precursor transcription factor expression is increased

The early pancreatic domain in zebrafish expresses *pdx1* and comprises an endocrine progenitor pool marked by the transcription factor *sox4b* (Biemar et al., 2001; Mavropoulos et al., 2005; Soyer et al., 2010; Tiso et al., 2009). The Sox4b$^+$ population appears to be distinct from hormone$^+$ cells at 24 hpf (Soyer et al., 2010). To identify whether the endocrine progenitor/precursor pool could be affected with the loss of Tm4sf4 function, we analyzed the progenitor markers *pdx1* and *sox4b* mRNA levels at 24 hpf. Interestingly, both *pdx1* and *sox4b* levels were significantly increased 1.4- and 1.5-fold, respectively (Fig. 6A-D), in embryos with reduced *tm4sf4* (Fig. 4Q). An expanded endocrine precursor pool could explain the increase of α and β cells, but a similar increase in δ and ε cells would also be expected. Instead, we observed a decrease in *ghrelin*$^+$ (ε) cells (Fig. 4K-M, Fig. 5E) and, although we observe subtle increases and decreases in *somatostatin* mRNA levels by qRT-PCR, we were unable to detect any noticeable variation in *somatostatin* mRNA or cell numbers by ISH (Fig. 4N-P) or immunofluorescence (data not shown). It remains possible that zebrafish *tm4sf4* can coordinate regulation of *pdx1* and *sox4b* expression levels within endocrine precursors, which could affect specific islet cell fate competency (Fukuda et al., 2008; Johansson et al., 2007; Wang et al., 2010). Alternatively, as Pdx1 is also expressed in β cells and expression of *sox4b* in a small subset of β cells at 20 hpf has been described (Mavropoulos et al., 2005), the increase in *pdx1* and *sox4b* expression might be secondary to the increase in β cell numbers at 24 hpf. However, we were unable to detect any *sox4b*$^+$ *insulin*$^+$ double-positive cells in either uninjected or Tm4MO embryos at 20 hpf (data not shown), suggesting that the increase in *sox4b* is independent of increased β cell numbers.

Tm4sf4 alters cell morphology and inhibits migration

We have determined that Ngn3$^+$ endocrine progenitor cells in mice are enriched with *Tm4sf4* (Fig. 2B). Ngn3 can drive EMT in endocrine progenitors, resulting in Snail2 (Snai2 – Mouse Genome Informatics) expression and a change in polarity preceding delamination, migration and differentiation into the five islet cell types (Gouzi et al., 2011; Kim and MacDonald, 2002; Pictet and Rutter, 1972; Rukstalis and Habener, 2007; Rutter et al., 1964). A gap remains in our understanding of the mechanisms linking transcriptional control to cell behaviors crucial for islet development. Interestingly, tetraspanin and L6 domain family members have been implicated in migration and adhesion in many

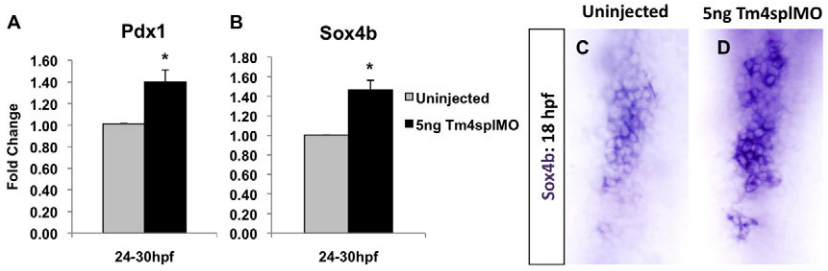

Fig. 6. *pdx1* and *sox4b* expression are increased in *tm4sf4* morphant zebrafish embryos.
(**A**,**B**) mRNA levels were measured at 24-30 hpf comparing uninjected embryos (gray) and *tm4sf4* morphants (black) for *pdx1* (A) and *sox4b* (B) by qRT-PCR. Error bars represent s.e.m. *P<0.05. (**C**,**D**) *sox4b* expression pattern was analyzed by in situ hybridization at 18 hpf.

tissues (Hemler, 2005; Wright et al., 2000). To analyze the functional role of Tm4sf4 in different cellular processes, we took advantage of in vitro cell culture systems to overexpress and knockdown Tm4sf4. To confirm the cellular context of *Tm4sf4* expression in vitro we first compared mRNA levels in several differentiated mouse pancreatic cell lines; mPacL20 (pancreatic duct cell, Nkx2.2^{-}), αTC1 (α cell, Nkx2.2^{+}) and βTC3 (β cell, Nkx2.2^{+}) cells (Gasa et al., 2004; Yoshida and Hanahan, 1994). Consistent with the high levels of ductal staining in the mouse (Fig. 1E,F,H,I), we found that *Tm4sf4* is expressed in the ductal mPacL20 cells that lack Nkx2.2, but is undetectable in αTC1 cells and expressed at very low levels in βTC3 cells (see Fig. S4 in the supplementary material).

To determine the intracellular localization of Tm4sf4, we overexpressed a Tm4sf4-FLAG fusion protein in NIH 3T3 and 293T fibroblast cells. As would be expected for an L6 domain tetraspanin molecule, Tm4sf4-FLAG protein was localized to the membrane and was apparent in vesicles (cytoplasmic punctae) (Fig. 7B). In addition, we observed that cells expressing Tm4sf4-FLAG displayed a striking cell morphological phenotype that was characterized by a multitude of filipodial cell protrusions that were not present in the mock-transfected controls (Fig. 7B). Not only did Tm4sf4-FLAG^{+} cells have more protrusions, but a large number of very thin filipodia appeared to be consistently concentrated on one edge of the cell. Frequently, multiple filipodial remnants also appeared to be detached or 'ripped' from the cell body (Fig. 7B,C). Membrane ripping has been shown to occur during slower fibroblast and keratinocyte migration where Integrin^{+} cell remnants are thought to provide a track for subsequent cell attachments (Bard and Hay, 1975; Chen, 1981; Kirfel et al., 2003; Palecek et al., 1998). Based on the cell morphological changes resulting from Tm4sf4-FLAG overexpression, we hypothesized that Tm4sf4 might act to stabilize cell protrusions and matrix contacts, resulting in migratory defects.

To test whether Tm4sf4 has a role in migration, we performed directed migration assays in Boyden chambers using both overexpression of Tm4sf4-FLAG in 293T cells, and knockdown of *Tm4sf4* in mPacL20 cells using siRNA technology. Using this assay, we determined Tm4sf4-FLAG overexpression in 293T cells (data not shown) or mPacL20 cells (Fig. 7F) caused a significant reduction in directed cellular migration (Fig. 7G). Conversely, we discovered that ~70% knockdown of endogenous *Tm4sf4* in mPacL20 cells (Fig. 7D) led to a significant increase in migrating cells (Fig. 7E). Based on these results, we believe that Tm4sf4 probably functions to inhibit cell detachment and/or cell migration, a crucial mechanism during islet morphogenesis and differentiation.

Directed cell migration requires alterations in the actin cytoskeleton organization and, therefore, we analyzed whether Tm4sf4 affects F-actin organization. NIH3T3 cells that overexpress Tm4sf4-FLAG (Fig. 8A, arrow) had more disorganized F-actin stress fibers emanating from an intense nucleation site. NIH3T3 and 293T cells that overexpress Tm4sf4-FLAG (Fig. 8A-C, arrows) exhibited a loss of defined cortical F-actin at the cell boundaries compared with that of characteristic lamellipodia in Tm4sf4^{-} cells (Fig. 8A-C, arrowheads). Instead, F-actin appeared to be more concentrated in the many filipodial extensions and cell protrusions of the less migratory cells expressing Tm4sf4-FLAG (Fig. 8C). mPacL20 cells endogenously expressing *Tm4sf4* displayed a variety of morphologies (Fig. 8D-F). However, upon treatment with siTm4sf4, threefold more cells within the population spread broadly in all directions with pronounced cortical F-actin and lamellipodial cell boundaries (Fig. 8G-I,K). In addition, cells with presumably lower levels of Tm4sf4 harbored more robust F-actin stress fibers and multiple cytoskeleton nucleation sites (Fig. 8G-I) than was seen in siControl cells.

The Rho family of GTPases (RhoA, Rac1, Cdc42) is known to regulate actin cytoskeleton organization and direct cellular migration and polarity. To identify whether Tm4sf4 dependent inhibition of migration requires Rho family GTPase activity, we first treated siControl or siTm4sf4 mPacL20 cells with the pan-Rho-GTPase inhibitor toxinB at 0.2 or 0.4 μg/ml, which repressed the migration induced by loss of *Tm4sf4* (Fig. 8L). To determine which Rho pathway Tm4sf4 might be involved with, we also treated siControl or siTm4sf4 cells with more specific pharmacological effectors: a Rac/Cdc42 activator, RhoA/B/C

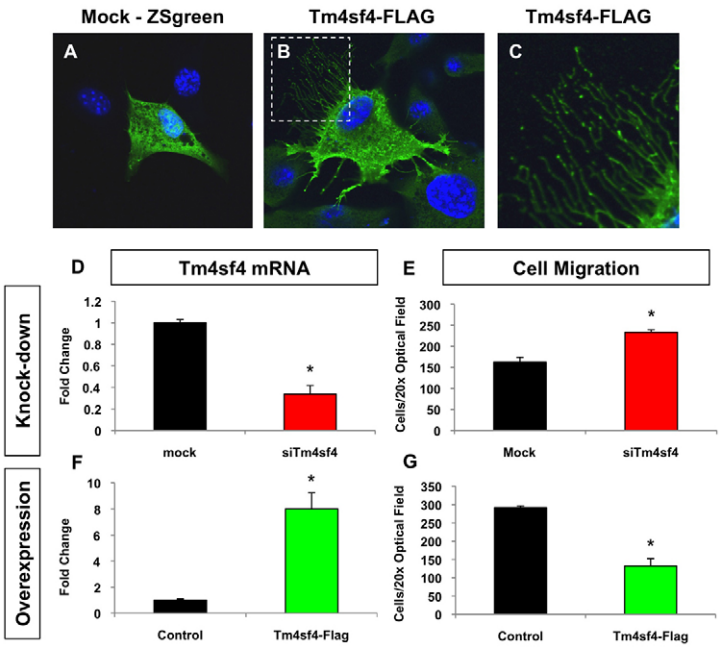

Fig. 7. Tm4sf4 alters cell morphology and inhibits cell migration. (**A-C**) Cell morphology was analyzed in mock/ZSgreen (A) and Tm4sf4-FLAG (B,C) transfected (green) NIH 3T3 cells. Nuclei were stained with DAPI and confocal images were acquired at 63×. C shows an enlargement of the boxed area in B. (**D-G**) Number of cells migrated in Boyden chamber assays compared with mock transfected cells when endogenous *Tm4sf4* is knocked down in mPacL20 ductal epithelial cells (D,E) or when Tm4sf4-FLAG is overexpressed in mPacL20 cells (F,G). Error bars represent s.e.m. **P*<0.05.

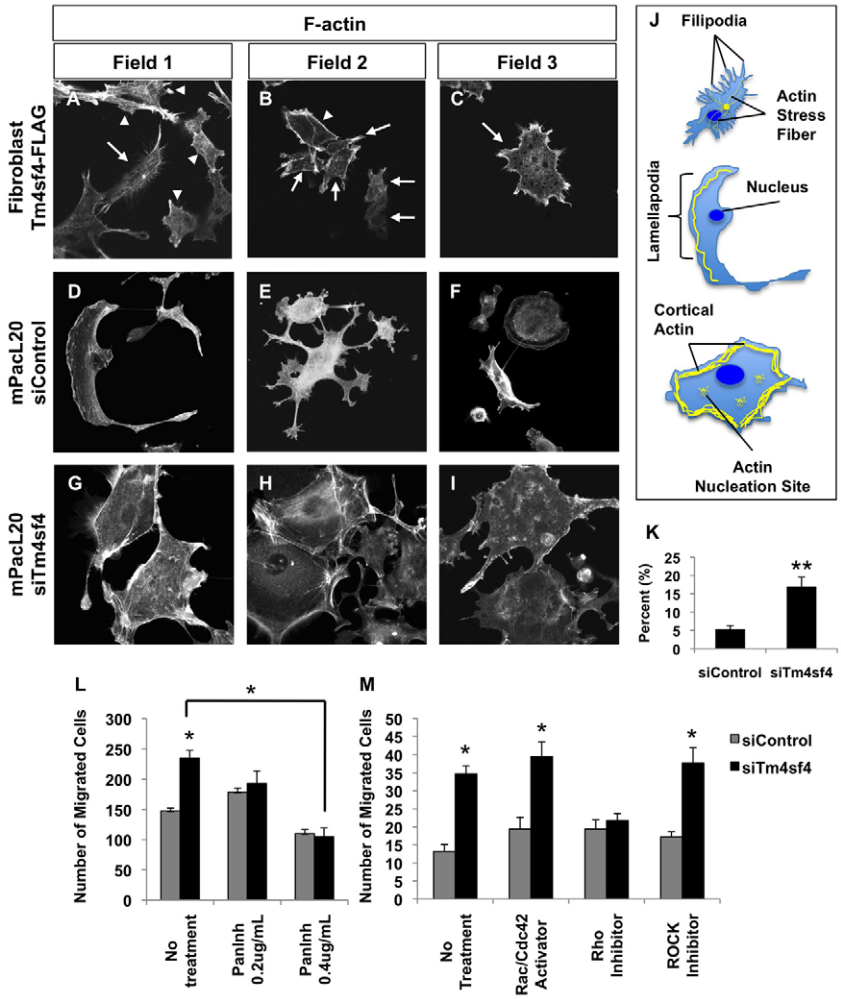

Fig. 8. Tm4f4 disrupts actin organization and migration through a ROCK-independent Rho GTPase pathway. (**A-I**) F-actin localization and organization was analyzed by rhodamine phalloidin staining in NIH 3T3 fibroblast (A) and 293T fibroblast (B,C) cells expressing (arrows) or not expressing (arrowheads) Tm4sf4-FLAG, as well as in mPacL20 ductal epithelial cells transfected with control siRNA (D-F) or siTm4sf4 (G-I). Confocal magnification 63×. (**J**) Schematic depicting cytoskeletal actin structures (yellow) affected by Tm4sf4. (**K**) Percentage of mPacL20 cells exhibiting the phenotype displayed in G-I. (**L**,**M**) Nuclei positive cells migrated in Boyden chamber assays were compared in siControl (gray) and siTm4sf4 (black) transfected cells 16 hours after cells were treated with Rho family GTPase modulators. Error bars represent s.e.m. **P*<0.05, ***P*<0.01.

inhibitor or a Rho kinase (ROCK) inhibitor. None of the drug treatments significantly affected normal siControl mPacL20 cell migration (Fig. 8M) regardless of visual perturbations to the actin cytoskeleton (see Fig. S5 in the supplementary material). Interestingly, the only pharmacological modulator to inhibit the increased migration resulting from a loss in *Tm4sf4* expression was the cell-permeable Rho inhibitor, C3 Transferase (Fig. 8M). Importantly, inhibition of the downstream effector of Rho, ROCK, did not suppress the increased migration caused by loss of *Tm4sf4* (Fig. 8M). Rho can also modulate the mammalian Diaphenous-related (mDia) formin pathway, which has been shown to localize in the lamella of migrating cells and is important for the stabilization of cortical actin, focal adhesion turnover and, thus, migration velocity (Gupton et al., 2007). Our data suggests that Tm4sf4 inhibits Rho activity independent of ROCK and could affect migration through the mDia/formin pathway.

DISCUSSION

Nkx2.2$^{-/-}$ mice completely lack β cells and lack the majority of their α cells, which are replaced by an increased ghrelin^{+} cell population. The mechanism by which *Nkx2.2* provides proper cell specification remains unknown. In previous studies, we identified *Tm4sf4* as a novel direct target of Nkx2.2 that is markedly increased in *Nkx2.2*$^{-/-}$ pancreata (Anderson et al., 2009b; Hill et al., 2011). In this study, we have confirmed that *Tm4sf4* is regulated by Nkx2.2 as early as e10.5 during pancreas organogenesis and that Ngn3^{+} endocrine progenitor cells are enriched with *Tm4sf4*. In the zebrafish model, *tm4sf4* inhibits α and β cell specification, but appears to be necessary for ε cell fates. Therefore, the *tm4sf4* morphant phenotype and *Nkx2.2*$^{-/-}$ or *nkx2.2a* morphant phenotypes are reversed, suggesting that Tm4sf4 might be a crucial factor downstream of Nkx2.2 controlling cell fate decisions. In support of this idea, co-injection of Nkx2.2atgMO and Tm4splMO into 1- to 4-cell stage zebrafish embryos causes a phenotype intermediate to wild-type and *tm4sf4* morphant embryos and suppresses the *nkx2.2a* morphant phenotype when analyzing *insulin* and *ghrelin* levels (Fig. 9A,B). Our data provides evidence to support the idea that Tm4sf4 lies downstream of Nkx2.2 and that its aberrant upregulation contributes to the *Nkx2.2*$^{-/-}$ phenotype.

Not surprisingly, the increase in β cells and decrease of ε cells resulting from loss of Tm4sf4 function were restricted to the pancreas. However, we observed that, in addition to increased α cells in the pancreas, transient *glucagon*$^{+}$ cells were present more posteriorly along the ventral midline in response to the reduction in *tm4sf4* in 20.5 hpf embryos. The ectopic *glucagon*$^{+}$ cells are located in a thin layer of endoderm that will later become the primitive gut (Ng et al., 2005; Wallace and Pack, 2003). Interestingly, the ectopic glucagon^{+} cells are localized in a pattern reminiscent of Tg[*nkx2.2a*:mEGFP]$^{+}$ cells that appear later during development of the posterior gut at 52 hpf (Ng et al., 2005). *Nkx2.2* is expressed in the mouse intestine between e14.5 and e15.5 at the onset of epithelial differentiation. *Nkx2.2*$^{-/-}$ mice harbor defects in

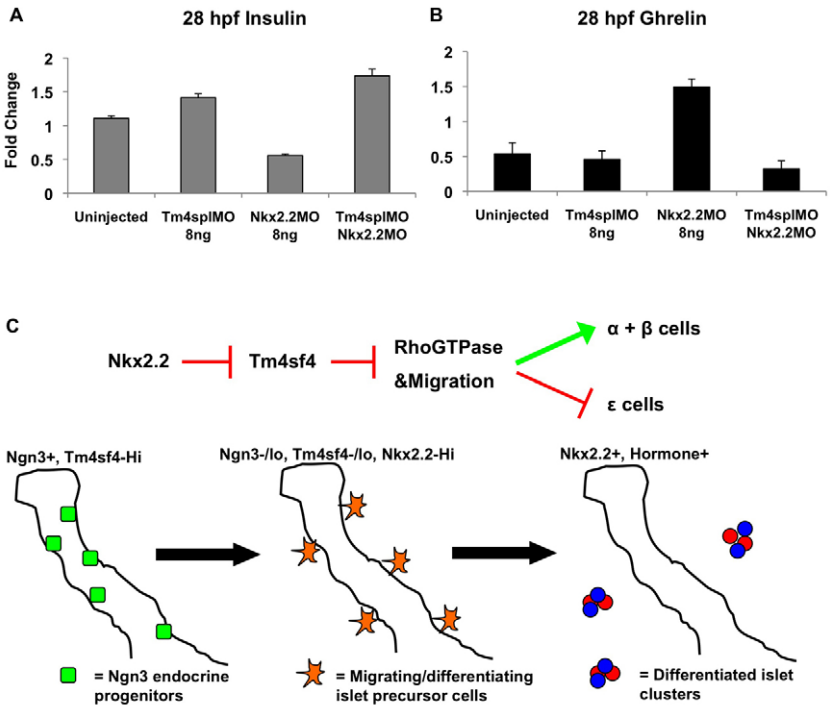

Fig. 9. Tm4sf4 is a critical factor downstream of Nkx2.2 and a model for a mechanism in endocrine islet cell fate specification. (**A**,**B**) Suppression analysis was performed in 28 hpf zebrafish by injecting antisense morpholinos against both *tm4sf4* and *nkx2.2a*. Differences in uninjected, single morphant and double morphant embryos were compared for *insulin* (A) and *ghrelin* (B) mRNA by qRT-PCR. Error bars represent s.e.m. (**C**) Our model proposes that Tm4sf4 is highly expressed within the Ngn3$^+$ progenitors inhibiting Rho GTPase-mediated detachment and migration. Nkx2.2 is required to downregulate Tm4sf4 and ultimately promote correct islet cell differentiation.

intestinal enteroendocrine cell fate decisions in addition to the more prominent pancreatic phenotype (Desai et al., 2008). A complete temporal analysis of enteroendocrine marker expression during zebrafish development is lacking, but PP$^+$ enteroendocrine cells appear to be restricted to the anterior intestine (bulb) and do not arise until 96 hpf (Wallace et al., 2005), whereas glucagon$^+$ somatostatin$^+$ double-positive enteroendocrine cells are restricted to the posterior intestine as early as 74 hpf (Ng et al., 2005). In support of previous observations, ectopic *glucagon*$^+$ cells are absent from the intestinal bulb domain adjacent to the pancreas; however, the appearance of *glucagon* in the primitive mid and posterior gut domains at 20.5 hpf in *tm4sf4* morphants occurs before intestinal tube morphogenesis is complete at 34 hpf. It has been reported that the earliest intestinal epithelium differentiation in zebrafish does not occur until 74 hpf (Wallace et al., 2005). We have only observed *tm4sf4* expression in liver, pancreas and intestinal bulb domains, so unless posterior intestinal *tm4sf4* is below detection limits, increased pancreatic α cells or aberrant intestinal bulb *glucagon*$^+$ cells are most likely to have differentiated outside the posterior intestine and migrated to the domain before undergoing cell death. Future experiments in both mouse and zebrafish models will allow us to investigate how Tm4sf4 might function in the pancreas and primitive gut.

In this study, we have shown that Tm4sf4 inhibits migration of both pancreatic ductal cells and non-pancreatic fibroblasts. Several L6 family members, *Tm4sf1* and *Tm4sf5*, are implicated in cell adhesion and migration during tumor progression and metastasis (Lee et al., 2008; Lee et al., 2006; Lekishvili et al., 2008; Muschel and Gal, 2008). *Tm4sf4* is involved in intestinal progenitor cell adhesion and migration during differentiation of intestinal crypt cells (Diosdado et al., 2004; Wice and Gordon, 1995). Recently in *Xenopus*, *Tm4sf3* was described to regulate dorsal and ventral pancreatic bud fusion and ventral bud cell migration, and independently appeared to inhibit ventral β cell differentiation (Jarikji et al., 2009). We believe Tm4sf4 plays a role during endocrine pancreas specification, promoting progenitor cell adhesion to the ductal epithelium and inhibiting migration of the differentiating Ngn3$^+$ population. As further evidence of an adhesion/migration role for Tm4sf4, we have observed that in *Nkx2.2*$^{-/-}$ mice (high *Tm4sf4*) the increased ghrelin$^+$ cell population form tight clusters that are strictly associated with the ductal epithelium (see Fig. S6 in the supplementary material). Although some wild-type ghrelin$^+$ ε cells are near pancreatic ducts at e16.5, ε cells are normally found distributed further from the local ductal environment within the migrating islets (see Fig. S6 in the supplementary material). It is possible that the loss of Nkx2.2 and subsequent upregulation of *Tm4sf4* impairs delamination and migration of the differentiating endocrine progenitors away from the ductal epithelium. This would suggest that α and β cell differentiation programs might be inhibited by prolonged exposure to the ductal environment, whereas this environment favors ε cell differentiation.

In support of this hypothesis, when *nkx2.2a* expression is knocked down in zebrafish, we not only see an increase in *tm4sf4* and decreased β cells (Pauls et al., 2007) (Fig. 3G,H; see Fig. S7 in the supplementary material), but also multiple small clusters of *insulin*-expressing cells that do not aggregate to form a primary islet (see Fig. S7 in the supplementary material). These data imply that *nkx2.2a* morphant β cells have defects in cell migration, in addition to β cell fate initiation, which might correlate with the increase in *tm4sf4* expression. A previous study in zebrafish showed that Wnt5a/Fz-2 (Fzd2 – Zebrafish Information Network) signaling was critical for β cell migration and islet formation (Kim et al., 2005). Recently, the tetraspanin Tspan12 has been shown to interact with Fzd4 and increase β-catenin signaling, crucial for proper retinal vasculature development (Junge et al., 2009). It is possible that Tm4sf4 might have a role in coordinating Wnt signaling and migration during endocrine pancreas specification.

Downstream of the non-canonical Wnt pathway lie the Rho-GTPase family of proteins (Rho, Rac, Cdc42) that modulate actin cytoskeleton, cell polarity, and migration. The cell migration

regulator, Rac1, was recently shown to regulate E-cadherin associated cell adhesion and subsequent migration of pancreatic β cells, presumably through actin remodeling (Kesavan et al., 2009). Our results have shown that Tm4sf4, which is highly expressed in the endocrine progenitors, appears to inhibit migration in a Rho GTPase (RhoA, RhoB, RhoC) dependent manner, allowing sustained contact with the ductal environment and affecting cell fate decisions. RhoA activity is mediated through downstream effectors ROCK and mDia. Multiple mDia genes have been implicated in driving migration during development and disease by promoting actin-rich cell protrusions and membrane blebbing (DeWard et al., 2010). Our data suggests that Tm4sf4 might inhibit cell migration via inhibition of an mDia-dependent Rho signaling pathway and not through ROCK. Interestingly, another member of the Rho-GTPase family, Cdc42, has been shown to control pancreatic tubulogenesis of the ducts and to maintain cell polarity. Pancreas-specific knockout of *Cdc42* led to a disrupted ductal architecture/microenvironment that results in fewer differentiated α and β cells (Kesavan et al., 2009). We believe that Tm4sf4 is involved in coordinating extracellular cues, cell migration and differentiation specifically within the endocrine pancreas domain.

Conclusion

In vivo, loss of Tm4sf4 function results in an increase in both α and β cell specification and inhibition of ε cell fates. In vitro studies demonstrate that Tm4sf4 promotes increased filipodia and inhibits cell migration mediated through ROCK-independent Rho-GTPase activity. Based on these complementary experimental approaches, we have developed a model whereby endocrine progenitor cells initially express high levels of *Tm4sf4*, which is downregulated by elevated expression of Nkx2.2. Once Tm4sf4 function is diminished, the endocrine progenitors detach from the surrounding epithelial ducts, actively rearrange the actin cytoskeleton and begin to delaminate, migrate and differentiate (Fig. 9C). We believe that *Tm4sf4* functions to inhibit β and α cell specification within the $Ngn3^{+}$ progenitors prior to islet precursor stages. It remains possible that Tm4sf4 could play a later role as a component of signaling pathways to drive cell fate switching independent of cell migration. We will need to utilize mouse model systems to take advantage of conditional knockout and overexpression technology to answer these types of questions confidently. Tm4sf4 promises to become a potential target for small molecule or function-blocking therapies that might provide an avenue to promote and activate quiescent pancreas progenitors in an in vivo or ex vivo environment.

Acknowledgements

We thank Lee Niswander and David Clouthier (UCAMC) for the use of their microscopes and tissue culture equipment; Christopher Wright (Vanderbilt University) for ISH probes; Ryan Anderson and Didier Stainier (UCSF) for transgenic zebrafish; Morgan Singleton for zebrafish line maintenance; Christina Chao for ISH troubleshooting; and Randall Wong/UCAMC BDC DERC Molecular Core for the use of the ABI 7000. We thank Shouhong Xuan for providing the Flag-tagged Tm4sf4 construct. We thank Teresa Mastracci, Kristi Lamonica and Davalyn Powell for critical reading of the manuscript. This project was supported by the NIDDK Beta Cell Biology Consortium (BCBC) grant U01 DK0272504 (L.S. and K.B.A.) and a BCBC Collaborative Bridging Project grant U19 DK0724473 (L.S., K.R.A. and K.B.A.). Deposited in PMC for release after 12 months.

Competing interests statement

The authors declare no competing financial interests.

Supplementary material

Supplementary material for this article is available at
http://dev.biologists.org/lookup/suppl/doi:10.1242/dev.058693/-/DC1

References

Anderson, K. R., Torres, C. A., Solomon, K., Becker, T. C., Newgard, C. B., Wright, C. V., Hagman, J. and Sussel, L. (2009a). Cooperative transcriptional regulation of the essential pancreatic islet gene NeuroD1 (beta2) by Nkx2.2 and neurogenin 3. *J. Biol. Chem.* **284**, 31236-31248.

Anderson, K. R., White, P., Kaestner, K. H. and Sussel, L. (2009b). Identification of known and novel pancreas genes expressed downstream of Nkx2.2 during development. *BMC Dev. Biol.* **9**, 65.

Bard, J. B. and Hay, E. D. (1975). The behavior of fibroblasts from the developing avian cornea. Morphology and movement in situ and in vitro. *J. Cell Biol.* **67**, 400-418.

Biemar, F., Argenton, F., Schmidtke, R., Epperlein, S., Peers, B. and Driever, W. (2001). Pancreas development in zebrafish: early dispersed appearance of endocrine hormone expressing cells and their convergence to form the definitive islet. *Dev. Biol.* **230**, 189-203.

Chen, W. T. (1981). Mechanism of retraction of the trailing edge during fibroblast movement. *J. Cell Biol.* **90**, 187-200.

Desai, S., Loomis, Z., Pugh-Bernard, A., Schrunk, J., Doyle, M. J., Minic, A., McCoy, E. and Sussel, L. (2008). Nkx2.2 regulates cell fate choice in the enteroendocrine cell lineages of the intestine. *Dev. Biol.* **313**, 58-66.

DeWard, A. D., Eisenmann, K. M., Matheson, S. F. and Alberts, A. S. (2010). The role of formins in human disease. *Biochim. Biophys. Acta* **1803**, 226-233.

Diosdado, B., Wapenaar, M. C., Franke, L., Duran, K. J., Goerres, M. J., Hadithi, M., Crusius, J. B., Meijer, J. W., Duggan, D. J., Mulder, C. J. et al. (2004). A microarray screen for novel candidate genes in coeliac disease pathogenesis. *Gut* **53**, 944-951.

Field, H. A., Dong, P. D., Beis, D. and Stainier, D. Y. (2003). Formation of the digestive system in zebrafish. II. Pancreas morphogenesis. *Dev. Biol.* **261**, 197-208.

Fukuda, A., Kawaguchi, Y., Furuyama, K., Kodama, S., Horiguchi, M., Kuhara, T., Kawaguchi, M., Terao, M., Doi, R., Wright, C. V. et al. (2008). Reduction of Ptf1a gene dosage causes pancreatic hypoplasia and diabetes in mice. *Diabetes* **57**, 2421-2431.

Gasa, R., Mrejen, C., Leachman, N., Otten, M., Barnes, M., Wang, J., Chakrabarti, S., Mirmira, R. and German, M. (2004). Proendocrine genes coordinate the pancreatic islet differentiation program in vitro. *Proc. Natl. Acad. Sci. USA* **101**, 13245-13250.

Gittes, G. K. (2009). Developmental biology of the pancreas: a comprehensive review. *Dev. Biol.* **326**, 4-35.

Gouzi, M., Kim, Y. H., Katsumoto, K., Johansson, K. and Grapin-Botton, A. (2011). Neurogenin3 initiates stepwise delamination of differentiating endocrine cells during pancreas development. *Dev. Dyn.* **240**, 589-604.

Gupton, S. L., Eisenmann, K., Alberts, A. S. and Waterman-Storer, C. M. (2007). mDia2 regulates actin and focal adhesion dynamics and organization in the lamella for efficient epithelial cell migration. *J. Cell Sci.* **120**, 3475-3487.

Hemler, M. E. (2005). Tetraspanin functions and associated microdomains. *Nat. Rev. Mol. Cell Biol.* **6**, 801-811.

Hemler, M. E. (2008). Targeting of tetraspanin proteins-potential benefits and strategies. *Nat. Rev. Drug Discov.* **7**, 747-758.

Hill, J. T., Anderson, K. R., Mastracci, T. L., Kaestner, K. H. and Sussel, L. (2011). Novel computational analysis of protein binding array data identifies direct targets of Nkx2.2 in the pancreas. *BMC Bioinformatics* **12**, 62.

Jarikji, Z., Horb, L. D., Shariff, F., Mandato, C. A., Cho, K. W. and Horb, M. E. (2009). The tetraspanin Tm4sf3 is localized to the ventral pancreas and regulates fusion of the dorsal and ventral pancreatic buds. *Development* **136**, 1791-1800.

Johansson, K. A., Dursun, U., Jordan, N., Gu, G., Beermann, F., Gradwohl, G. and Grapin-Botton, A. (2007). Temporal control of neurogenin3 activity in pancreas progenitors reveals competence windows for the generation of different endocrine cell types. *Dev. Cell* **12**, 457-465.

Jorgensen, M. C., Ahnfelt-Ronne, J., Hald, J., Madsen, O. D., Serup, P. and Hecksher-Sorensen, J. (2007). An illustrated review of early pancreas development in the mouse. *Endocr. Rev.* **28**, 685-705.

Junge, H. J., Yang, S., Burton, J. B., Paes, K., Shu, X., French, D. M., Costa, M., Rice, D. S. and Ye, W. (2009). TSPAN12 regulates retinal vascular development by promoting Norrin- but not Wnt-induced FZD4/beta-catenin signaling. *Cell* **139**, 299-311.

Kao, Y. R., Shih, J. Y., Wen, W. C., Ko, Y. P., Chen, B. M., Chan, Y. L., Chu, Y. W., Yang, P. C., Wu, C. W. and Roffler, S. R. (2003). Tumor-associated antigen L6 and the invasion of human lung cancer cells. *Clin. Cancer Res.* **9**, 2807-2816.

Kesavan, G., Sand, F. W., Greiner, T. U., Johansson, J. K., Kobberup, S., Wu, X., Brakebusch, C. and Semb, H. (2009). Cdc42-mediated tubulogenesis controls cell specification. *Cell* **139**, 791-801.

Kim, H. J., Schleiffarth, J. R., Jessurun, J., Sumanas, S., Petryk, A., Lin, S. and Ekker, S. C. (2005). Wnt5 signaling in vertebrate pancreas development. *BMC Biol.* **3**, 23.

Kim, S. K. and MacDonald, R. J. (2002). Signaling and transcriptional control of pancreatic organogenesis. *Curr. Opin. Genet. Dev.* **12**, 540-547.
Kimmel, C. B., Ballard, W. W., Kimmel, S. R., Ullmann, B. and Schilling, T. F. (1995). Stages of embryonic development of the zebrafish. *Dev. Dyn.* **203**, 253-310.
Kinkel, M. D. and Prince, V. E. (2009). On the diabetic menu: zebrafish as a model for pancreas development and function. *BioEssays* **31**, 139-152.
Kinkel, M. D., Eames, S. C., Alonzo, M. R. and Prince, V. E. (2008). Cdx4 is required in the endoderm to localize the pancreas and limit beta-cell number. *Development* **135**, 919-929.
Kirfel, G., Rigort, A., Borm, B., Schulte, C. and Herzog, V. (2003). Structural and compositional analysis of the keratinocyte migration track. *Cell Motil. Cytoskeleton* **55**, 1-13.
Lee, C. S., Perreault, N., Brestelli, J. E. and Kaestner, K. H. (2002). Neurogenin 3 is essential for the proper specification of gastric enteroendocrine cells and the maintenance of gastric epithelial cell identity. *Genes Dev.* **16**, 1488-1497.
Lee, S. A., Lee, S. Y., Cho, I. H., Oh, M. A., Kang, E. S., Kim, Y. B., Seo, W. D., Choi, S., Nam, J. O., Tamamori-Adachi, M. et al. (2008). Tetraspanin TM4SF5 mediates loss of contact inhibition through epithelial-mesenchymal transition in human hepatocarcinoma. *J. Clin. Invest.* **118**, 1354-1366.
Lee, S. Y., Kim, Y. T., Lee, M. S., Kim, Y. B., Chung, E., Kim, S. and Lee, J. W. (2006). Focal adhesion and actin organization by a cross-talk of TM4SF5 with integrin alpha2 are regulated by serum treatment. *Exp. Cell Res.* **312**, 2983-2999.
Lekishvili, T., Fromm, E., Mujoomdar, M. and Berditchevski, F. (2008). The tumour-associated antigen L6 (L6-Ag) is recruited to the tetraspanin-enriched microdomains: implication for tumour cell motility. *J. Cell Sci.* **121**, 685-694.
Liu, Z., Zhao, M., Yokoyama, K. K. and Li, T. (2001). Molecular cloning of a cDNA for rat TM4SF4, a homolog of human il-TMP (TM4SF4), and enhanced expression of the corresponding gene in regenerating rat liver(1). *Biochim. Biophys. Acta* **1518**, 183-189.
Marken, J. S., Schieven, G. L., Hellstrom, I., Hellstrom, K. E. and Aruffo, A. (1992). Cloning and expression of the tumor-associated antigen L6. *Proc. Natl. Acad. Sci. USA* **89**, 3503-3507.
Mavropoulos, A., Devos, N., Biemar, F., Zecchin, E., Argenton, F., Edlund, H., Motte, P., Martial, J. A. and Peers, B. (2005). sox4b is a key player of pancreatic alpha cell differentiation in zebrafish. *Dev. Biol.* **285**, 211-223.
Muller-Pillasch, F., Wallrapp, C., Lacher, U., Friess, H., Buchler, M., Adler, G. and Gress, T. M. (1998). Identification of a new tumour-associated antigen TM4SF5 and its expression in human cancer. *Gene* **208**, 25-30.
Murtaugh, L. C. (2008). The what, where, when and how of Wnt/beta-catenin signaling in pancreas development. *Organogenesis* **4**, 81-86.
Muschel, R. J. and Gal, A. (2008). Tetraspanin in oncogenic epithelial-mesenchymal transition. *J. Clin. Invest.* **118**, 1347-1350.
Ng, A. N., de Jong-Curtain, T. A., Mawdsley, D. J., White, S. J., Shin, J., Appel, B., Dong, P. D., Stainier, D. Y. and Heath, J. K. (2005). Formation of the digestive system in zebrafish: III. Intestinal epithelium morphogenesis. *Dev. Biol.* **286**, 114-135.
Oliver-Krasinski, J. M. and Stoffers, D. A. (2008). On the origin of the beta cell. *Genes Dev.* **22**, 1998-2021.
Palecek, S. P., Huttenlocher, A., Horwitz, A. F. and Lauffenburger, D. A. (1998). Physical and biochemical regulation of integrin release during rear detachment of migrating cells. *J. Cell Sci.* **111**, 929-940.
Parsons, M. J., Pisharath, H., Yusuff, S., Moore, J. C., Siekmann, A. F., Lawson, N. and Leach, S. D. (2009). Notch-responsive cells initiate the secondary transition in larval zebrafish pancreas. *Mech. Dev.* **126**, 898-912.
Pauls, S., Zecchin, E., Tiso, N., Bortolussi, M. and Argenton, F. (2007). Function and regulation of zebrafish nkx2.2a during development of pancreatic islet and ducts. *Dev. Biol.* **304**, 875-890.
Pictet, R. and Rutter, W. J. (1972). *Development of the Embryonic Endocrine Pancreas*. Washington, DC: Williams and Wilkins.
Prado, C. L., Pugh-Bernard, A. E., Elghazi, L., Sosa-Pineda, B. and Sussel, L. (2004). Ghrelin cells replace insulin-producing beta cells in two mouse models of pancreas development. *Proc. Natl. Acad. Sci. USA* **101**, 2924-2929.
Puri, S. and Hebrok, M. (2010). Cellular plasticity within the pancreas – lessons learned from development. *Dev. Cell* **18**, 342-356.
Qiu, J., Liu, Z., Da, L., Li, Y., Xuan, H., Lin, Q., Li, F., Wang, Y., Li, Z. and Zhao, M. (2007). Overexpression of the gene for transmembrane 4 superfamily member 4 accelerates liver damage in rats treated with CCl4. *J. Hepatol.* **46**, 266-275.
Rukstalis, J. M. and Habener, J. F. (2007). Snail2, a mediator of epithelial-mesenchymal transitions, expressed in progenitor cells of the developing endocrine pancreas. *Gene Expr. Patterns* **7**, 471-479.
Rutter, W. J., Wessells, N. K. and Grobstein, C. (1964). Control of specific sythesis in the developing pancreas. *Natl. Cancer Inst. Monogr.* **13**, 51-65.
Rutter, W. J., Rajkumar, T., Penhoet, E., Kochman, M. and Valentine, R. (1968). Aldolase variants: structure and physiological significance. *Ann. N. Y. Acad. Sci.* **151**, 102-117.
Slack, J. M. (1995). Developmental biology of the pancreas. *Development* **121**, 1569-1580.
Soyer, J., Flasse, L., Raffelsberger, W., Beucher, A., Orvain, C., Peers, B., Ravassard, P., Vermot, J., Voz, M. L., Mellitzer, G. et al. (2010). Rfx6 is an Ngn3-dependent winged helix transcription factor required for pancreatic islet cell development. *Development* **137**, 203-212.
Storim, J., Friedl, P., Schaefer, B. M., Bechtel, M., Wallich, R., Kramer, M. D. and Reinartz, J. (2001). Molecular and functional characterization of the four-transmembrane molecule l6 in epidermal keratinocytes. *Exp. Cell Res.* **267**, 233-242.
Sussel, L., Kalamaras, J., Hartigan-O'Connor, D. J., Meneses, J. J., Pedersen, R. A., Rubenstein, J. L. and German, M. S. (1998). Mice lacking the homeodomain transcription factor Nkx2.2 have diabetes due to arrested differentiation of pancreatic beta cells. *Development* **125**, 2213-2221.
Thisse, C. and Thisse, B. (2008). High-resolution in situ hybridization to whole-mount zebrafish embryos. *Nat. Protoc.* **3**, 59-69.
Tiso, N., Moro, E. and Argenton, F. (2009). Zebrafish pancreas development. *Mol. Cell. Endocrinol.* **312**, 24-30.
Wallace, K. N. and Pack, M. (2003). Unique and conserved aspects of gut development in zebrafish. *Dev. Biol.* **255**, 12-29.
Wallace, K. N., Akhter, S., Smith, E. M., Lorent, K. and Pack, M. (2005). Intestinal growth and differentiation in zebrafish. *Mech. Dev.* **122**, 157-173.
Wang, S., Yan, J., Anderson, D. A., Xu, Y., Kanal, M. C., Cao, Z., Wright, C. V. and Gu, G. (2010). Neurog3 gene dosage regulates allocation of endocrine and exocrine cell fates in the developing mouse pancreas. *Dev. Biol.* **339**, 26-37.
White, P., May, C. L., Lamounier, R. N., Brestelli, J. E. and Kaestner, K. H. (2008). Defining pancreatic endocrine precursors and their descendants. *Diabetes* **57**, 654-668.
Wice, B. M. and Gordon, J. I. (1995). A tetraspan membrane glycoprotein produced in the human intestinal epithelium and liver that can regulate cell density-dependent proliferation. *J. Biol. Chem.* **270**, 21907-21918.
Wright, M. D., Ni, J. and Rudy, G. B. (2000). The L6 membrane proteins-a new four-transmembrane superfamily. *Protein Sci.* **9**, 1594-1600.
Yoshida, T. and Hanahan, D. (1994). Murine pancreatic ductal adenocarcinoma produced by in vitro transduction of polyoma middle T oncogene into the islets of Langerhans. *Am. J. Pathol.* **145**, 671-684.
Yunta, M. and Lazo, P. A. (2003). Tetraspanin proteins as organisers of membrane microdomains and signalling complexes. *Cell. Signal.* **15**, 559-564.
Zecchin, E., Filippi, A., Biemar, F., Tiso, N., Pauls, S., Ellertsdottir, E., Gnugge, L., Bortolussi, M., Driever, W. and Argenton, F. (2007). Distinct delta and jagged genes control sequential segregation of pancreatic cell types from precursor pools in zebrafish. *Dev. Biol.* **301**, 192-204.

Table S1. qRT-PCR primer and probe sequences

Gene symbol	Forward primer (5′-3′)	Reverse primer (5′-3′)	Probe (5′-3′)
Mouse			
Ngn3	GACGCCAAACTTACAAAG	GTCAGTGCCCAGATGT	CCTGCGCTTCGCCCACAACT
cyclophilin B (*Ppib*)	GCAAAGTTCTAGAGGGCATGGA	CCCGGCTGTCTGTCTTGGT	TGGTACGGAAGGTGGAG
Zebrafish			
β-*actin*	CATCAGGGTGTCATGGTTGGT	TCTCTTGCTCTGAGCCTCATCA	TGGGACAGAAAGACAGCTA
cp	GCTCCCAGCGGTAAAAACCT	CGCGCGGCTTCATCTT	ATTCAGAACAAAACCG
ghrelin	TCCTCAGTCCGACTCAGAAACC	GCTTCTCTTCTGCCCACTCTTG	AGGGTCGAAGGCCA
glucagon	AAGCGAGGAGACGATCCAAA	TCCAACACACACCAGCAAATG	ACATTTCATATCATCTCATCC
hhex	GGCGGCCAGGTTCGAT	CGAACTTCTTCTCCAGCTCGAT	CTCCAACGATCAAAC
insulin	GAGCCCCTTCTGGGTTTCC	AAGTCAGCCACCTCAGTTTCCT	TCCTCCTAAATCTGCC
nkx2.2a	AACCACGGACAGCATCCAAT	TTTGCGGACGTGTCTTGAGA	TCATTACACGGCCTGTCCGCGAA
pdx1	CACACGCACGCATGGAAA	TCCTCGGCCTCGACCATAT	CAGTGGACAGGCCCT
prox1	CGTGCTCTCAACATGCACTACA	GGAATCGCTCCGGAACCT	AAGGCCAACGATTTT
somatostatin	GCCAAACTCCGCCAACTTC	CTGGCGAGTTCCTGTTTTCC	ATCTCTCCTCAGCCCTG